J Mater Sci: Mater Med (2010) 21:2523–2531
DOI 10.1007/s10856-010-4110-9

# Effect of ceramic filler content on the mechanical and thermal behaviour of poly-L-lactic acid and poly-L-lactic-co-glycolic acid composites for medical applications

**Behzad Damadzadeh · Hamideh Jabari · Mikael Skrifvars · Karri Airola · Niko Moritz · Pekka K. Vallittu**

Received: 1 July 2009 / Accepted: 25 May 2010 / Published online: 15 June 2010

**Abstract** One main application of resorbable poly-L-lactic acid (PLLA) and poly-L-lactic-co-glycolic acid (PLGA) based materials is in medical implants. In this study composites were made from PLLA and PLGA with hydroxyapatite (HAp) respective $\beta$-tricalcium phosphate ($\beta$-TCP) fillers. The filler content and particle size were varied, and the thermal properties as well as the mechanical strength of the composites were investigated. The composites were made by an extrusion compounding process giving 2–2.5 mm diameter sized profiles. The results verified that the thermal stability of the composites was reasonable during the optimized compounding conditions. Scanning electron microscopy revealed that the fillers were well dispersed in the polymer matrices. The mechanical properties were improved by the addition of the fillers. The optimum mechanical properties for the extruded profiles were obtained with the HAp fillers. The E-modulus was increased from 3.3 to 4.6 GPa by addition of filler particles (30 wt%) whereas the flexural strength was reduced from 133 to 106 MPa.

B. Damadzadeh · H. Jabari · M. Skrifvars (✉) · K. Airola
School of Engineering, University of Borås, Allegatan 1, 501 90 Borås, Sweden
e-mail: mikael.skrifvars@hb.se

N. Moritz
Turku Clinical Biomaterials Centre, University of Turku, Itäinen Pitkäkatu 4B (PharmaCity), 205 20 Turku, Finland

P. K. Vallittu
Institute of Dentistry and BioCity Turku Biomaterials Research Program, University of Turku, 205 20 Turku, Finland

## 1 Introduction

Biomaterials are materials that constitute parts of medical implants, extracorporeal devices, and disposables that have been utilized in medicine, surgery, dentistry, and veterinary medicine as well as in every aspect of patient health care [1]. Since living tissues are combinations of different macromolecules and other components, biodegradable polymers are a highly feasible group of material from which biocompatible materials can be developed. The possess characteristics perfectly fitted for replacement, support, augmentation or fixation of living tissues [2, 3]. The main advantage and idea behind the development of biodegradable implants is the avoidance of repeat surgery for the removal of metal implants. Biodegradable polymers can be used as bone fractures fixation devices in orthopedic areas such as elbow, shoulder, knee, wrist and pelvis [4–6] due to their biocompatibility, biodegradability, non-toxicity, superior mechanical properties and processability. Poly lactic acid and poly glycolic acid polymers and their co-polymers are well-known bioabsorbable polymers due to containing similar chemical components to bone [7, 8].

Insufficient mechanical strength and osteoconductivity of these pure polymers have increased the interest in reinforcing them with particulate fillers such as hydroxyapatite and $\beta$-tricalcium phosphate [9]. By the addition of particulate fillers, the mechanical properties are expected to increase especially if the filler-polymer matrix adhesion enables load transfer from the matrix, and the fillers are able to prevent crack propagation through the composite.

Several methods have been introduced for combining polymers and ceramic fillers such as solution casting [10–17], co-precipitation [18] and melt extrusion [5, 9, 13, 14, 19, 20]. The latter is commonly used for processing polymeric implant composites [21]. The most critical issue in composite processing is to achieve homogenous mixing of the fillers resulting in their optimal dispersion and distribution. Furthermore, it is necessary to optimize the processing conditions to attain the best possible mechanical properties with no thermal degradation of the polymer due to the high processing temperature.

In this study a twin screw 15 $cm^3$ micro-compounder was used to mix poly-L-lactic acid (PLLA) and poly-L-lactic-co-glycolic acid (PLGA) with hydroxyapatite (HAp) and $\beta$-tricalciumphosphate ($\beta$-TCP). The composites were further extruded into rod-like profiles with a diameter of 2–2.5 mm. The effect of filler content (0–30 wt%) and filler particle size (200 nm to 50 μm) on the composite properties were investigated. Analytical techniques applied included solution viscosimetry, differential scanning calorimetry (DSC), thermal gravimetric analysis (TGA), three point bend testing and scanning electron microscopy (SEM).

The objective of this work was to improve the mechanical strength of melt-processed composites and for their use as biodegradable bone pins and fixture screws. The processing conditions must be optimized in order to minimize thermal degradation during the melt processing. Processing temperature, residence time and extruder screw rotational speed (rpm) were studied.

## 2 Experimental

### 2.1 Materials

The biopolymers selected as the matrix material were poly-L-lactide (PLLA) (Purasorb PL65) with inherent viscosity (i.v.) of 7.02 dl $g^{-1}$ supplied by PURAC biomaterials, the Netherlands, and poly-L-lactide-co-glycolide (PLGA) 85:15 (Resomer LG 855S) with inherent viscosity (i.v.) of 3.5 dl $g^{-1}$ supplied by Boehringer Ingelheim Pharma GmbH & Co. KG, Germany. Hydroxyapatite and $\beta$-tricalcium phosphate bioceramic additive fillers with different particle sizes were selected to reinforce the biopolymers. The filler suppliers and particle sizes are shown in Table 1. The filler particle size distributions were analyzed from SEM images as explained below. All materials were dried in vacuum at 40°C overnight, and then stored under vacuum.

**Table 1** Particle size and suppliers for used ceramic fillers

| Filler name | Particle size | Supplier |
|---|---|---|
| Hydroxyapatite | 0–50 μm | Berkeley Advanced Biomaterials, USA |
| Hydroxyapatite | 5 μm | Berkeley Advanced Biomaterials, USA |
| Hydroxyapatite | <200 nm | SIGMA ALDRICH, USA |
| $\beta$-Tricalciumphosphate | 0–50 μm | Berkeley Advanced Biomaterials, USA |

### 2.2 Melt extrusion method

The composites were prepared in a 15 $cm^3$ co-rotating twin screw microcompounder from DSM Xplore Research, the Netherlands. The processing temperatures were 180–190°C for the PLGA composites, and 215°C for the PLLA composites. Argon was used as purging gas to prevent oxidative degradation. The screw rotation speed was 20 rpm and residence time was selected to 2 min in order to minimize the risk of polymer thermal degradation. Before compounding the PLLA and PLGA granules were manually mixed with different filler weight additions. The feeding was done continuously through an upper funnel hopper. The materials were then extruded through a 2 mm diameter die equipped with an outside circular air cooler, and further drawn down to approximately 2–2.5 mm diameter profiles with the help of a moving conveyor belt. Profile specimens were then cut into different lengths, and stored under vacuum until characterisation. The processing conditions employed were selected based on previously performed experimental trials. For HAp, the filler content was 10, 20 and 30 wt% and the most interesting results were achieved for the 20 wt% content composites, this filler content was also selected for the $\beta$-TCP containing composite.

### 2.3 Thermal characterization

The polymer thermal characteristics were determined using a TA Instruments Q1000 differential scanning calorimeter (New Castle, DE, USA). Specimens weighing 7–10 mg were cut and placed in aluminium pans. The specimens were first heated from 0 to 200°C and then cooled to 0°C at heating rate 20°C $min^{-1}$ under nitrogen atmosphere. Two identical samples were analyzed for each prepared compounded composition. The glass transition temperature ($T_g$), melting point ($T_m$) recrystallization temperature ($T_c$) and melting heat of fusion ($\Delta H_m$) were obtained from the DSC curves. The degree of crystallinity ($X_c$) was calculated from the enthalpy of melting for 100% crystalline PLA (93.6 J $g^{-1}$) by using the following equation:

$$X_c = (\Delta H_m - \Delta H_c) \times 100/93.7$$

Thermo gravimetric analysis (TGA) studies were performed on TA Instruments Q500 system (New Castle, DE, USA). Experiments were performed in nitrogen atmosphere and specimens were run from 0 to 600°C at heating rate of 10°C $min^{-1}$. The thermal decomposition temperatures as well as the filler contents in the composites were determined from the TGA curves. The filler content was determined for composite samples taken during the continuous extrusion process. This was important as the filler loading might vary during the process.

### 2.4 Inherent viscosity

The pure polymers as well as the composite samples (approximately 0.1 g amounts of each) were dissolved in chloroform (99.99% purity, Fisher Scientific) by stirring with magnet stirrer for 3 days at room temperature. The solutions were then inserted into a capillary viscometer, which was placed in a thermostat water bath at 30°C for 15 min. The flow time of the polymer solution between the two marks in the capillary was recorded by a ViscoClock device (SCHOTT AG, Germany). The flow time for pure chloroform was measured as a reference. Four to six measurements were performed for each sample. The measured flow times were all within a range of ±0.3 s. The inherent viscosity (i.v.) was calculated using the following equation:

$$\text{i.v.} = (\ln V_r)/C$$

Here $V_r$ is the relative viscosity, or the flow time ratio of the polymer solution to the pure chloroform, and C is the polymer concentration having the unit of grams per decilitre.

### 2.5 Mechanical testing

Flexural strength and modulus of elasticity were measured by a three point bending test on a Lloyd LRX (Lloyd Instruments Ltd, Fareham, England) testing machine. A loading rate of 1 mm $\text{min}^{-1}$ was applied. For each sample composition 6–8 profile specimens were tested, and the average values and the standard deviations were calculated. The sample dimensions were 25 mm in length and 2–3 mm in diameter. The mechanical testing was done at room temperature in dry conditions.

### 2.6 Scanning electron microscopy (SEM)

The morphology of the fracture surface of all composites was studied using a JSM-5500 (JEOL Ltd., Tokyo, Japan) scanning electron microscope. Samples were cut in liquid nitrogen and the fractured surfaces were sputter coated with gold. An accelerating voltage of 15 kV and a working distance of 20 mm were used. The magnifications 500×, 800×, 1500× and 5000× were used, and the 1500× magnification was considered as the best in order to produce good resolved micrographs. To determine the particle size distributions for the used ceramic fillers these were imaged by SEM, and the obtained images were analysed by a CT-analyser software (Ver. 1.7.0.5, SkyScan NV, Belgium) to obtain particle size distributions. A frequency count of the data was done by OriginPro (Version 7.5 SR4, OriginLab Corp. USA) to give bar chart particle size distributions.

## 3 Results and discussion

### 3.1 Filler characterisation

The particle size distributions for the used fillers are shown in Fig. 1. The particle size distribution for the 0–50 µm HAp filler corresponds well with the supplier data. For the 5 µm HAp a rather large fraction of particles with sizes larger than 5 µm can be seen. The $\beta$-TCP filler particle size distribution deviates clearly from the supplier data, a very large fraction of the particles are bigger than 50 µm. It was not possible to analyse the HAp with reported size less than 200 nm, due to the small size. All analyzed fillers showed on the SEM micrographs spherical structures, with few defects, and no agglomerations.

### 3.2 Melt extrusion

The most optimal processing conditions were selected using the data from the DSC analysis, i.e. the melting temperature and the inherent viscosity. These properties are thermal indicators for polymer degradation. The adjustment of the compounder shear force was found as the most important parameter for optimal processing. A screw rotational velocity of 20 rpm was used for all processing runs. If the shear force decreased dramatically during the feeding process, it was obvious that polymer degradation has occurred. To overcome this problem, the running conditions had to be improved and the feeding time reduced. The degradation could then further be avoided by careful drying of the polymer granulates, as well as by the use of purging argon gas in the compounder barrel.

The feeding time of bioceramic fillers to both polymer matrices was reasonable short (less than 10 min), with the exception for the addition of the 0–50 µm HAp filler particles to the PLLA melt. This was probably related to the high inherent viscosity of the PLLA. The machine back-pressures were also close to the maximum possible pressure (8000 N) with exception to when the 200 nm size HAp fillers were added to PLLA. Typical extruded profiles are shown in Fig. 2. A colour variation depending on the filler loading could be seen for most of the profiles.

### 3.3 Degree of crystallinity and phase transitions

The glass transition temperatures, melting points, as well as the degrees of crystallinity are shown in Tables 2 and 3. The $T_g$ is a kinetic phenomenon which includes the

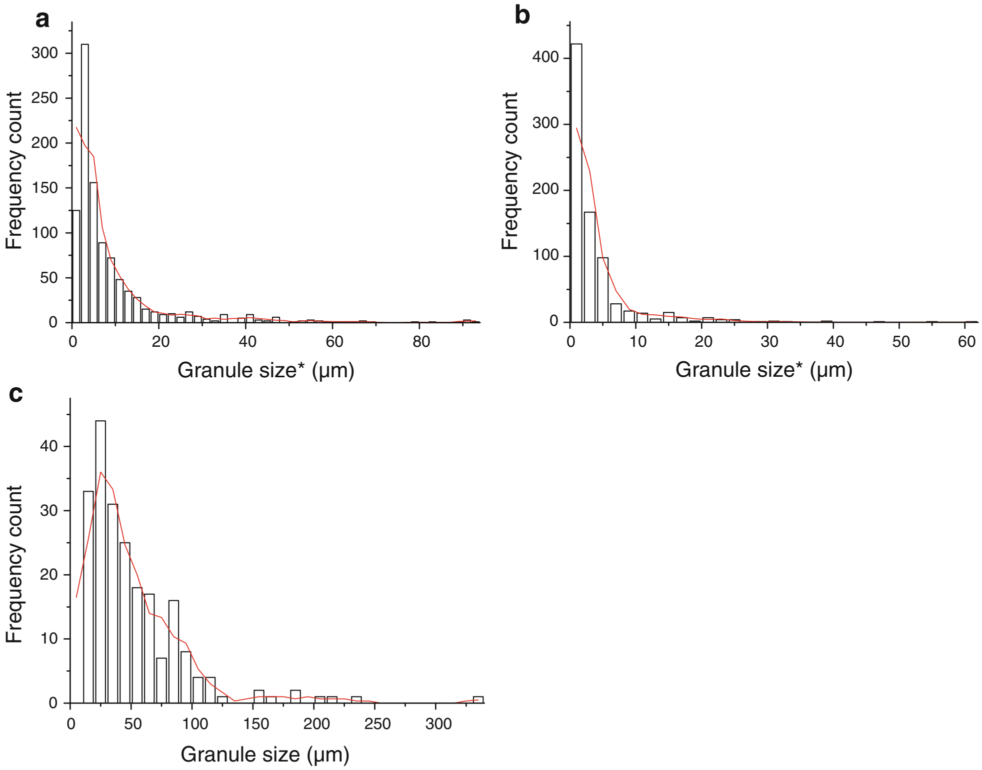

**Fig. 1** Analyzed particle size distributions for the used fillers. **a** 0–50 μm HAp, **b** 5 μm HAp, **c** 0–50 μm *β*-TCP

polymer viscoelasticity which, in turn, is affected by experimental conditions such as the thermal history of the specimen and the heating rate.

PLGA had a $T_g$ of around 59°C, and PLLA had a $T_g$ around 63°C, which corresponds well to values from the literature, considering the thermal history [22, 23]. The addition of fillers had no effect on the $T_g$ for both polymers, but the $T_m$ for the PLGA profile decreased with increased filler loading at the same compounding condition. The decrease in $T_m$ during compounding could be ascribed to the stress release of molecular chains during heating [9]. Although an increase in residence time caused a more homogeneous dispersion, with better contact between components, there was also the risk of polymer degradation, as indicated by a minor decrease in $T_m$ seen in the DSC results [13].

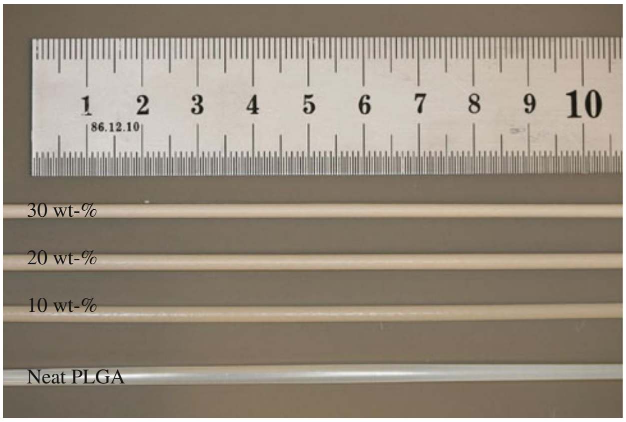

**Fig. 2** Typical obtained extruded profiles from PLGA and 5 μm HAp with different filler loading

**Table 2** Thermal properties of PLGA and ceramic fillers

| Filler conc. (wt%) | HAp (0–50 μm) | | | HAp (0–5 μm) | | | HAp (<200 nm) | | | *β*-TCP (0–50 μm) | | |
|---|---|---|---|---|---|---|---|---|---|---|---|---|
| | $T_g$ (°C) | $T_m$ (°C) | $\Delta H_m$ (J $g^{-1}$) | $T_g$ (°C) | $T_m$ (°C) | $\Delta H_m$ (J $g^{-1}$) | $T_g$ (°C) | $T_m$ (°C) | $\Delta H_m$ (J $g^{-1}$) | $T_g$ (°C) | $T_m$ (°C) | $\Delta H_m$ (J $g^{-1}$) |
| 0 | 59.25 | 159.75 | 14.67 | 59.25 | 159.75 | 14.67 | 59.25 | 159.75 | 14.67 | 59.25 | 159.75 | 15.65 |
| 10 | 59.84 | 156.86 | 15.84 | 59.58 | 156.72 | 19.96 | 59.94 | 156.68 | 15.29 | n.d. | n.d. | n.d. |
| 20 | 59.38 | 156.40 | 17.34 | 59.23 | 156.92 | 19.58 | 60.23 | 156.93 | 14.96 | 59.75 | 157.08 | 7.78 |
| 30 | 59.31 | 155.02 | 11.61 | 59.12 | 155.97 | 14.72 | 59.10 | 155.82 | 13.32 | n.d. | n.d. | n.d. |

**Table 3** Thermal properties of PLLA and ceramic fillers

| Filler conc. (wt%) | HAp (0–50 μm) | | | | HAp (0–5 μm) | | | |
|---|---|---|---|---|---|---|---|---|
| | $T_g$ (°C) | $T_m$ (°C) | Crystallinity (%) | $\Delta H_m$ (J $g^{-1}$) | $T_g$ (°C) | $T_m$ (°C) | Crystallinity (%) | $\Delta H_m$ (J $g^{-1}$) |
| 0 | 63.25 | 176.93 | 1.2 | 32.47 | 63.25 | 176.93 | 1.20 | 32.47 |
| 10 | 63.37 | 176.89 | 1.68 | 32.75 | 63.14 | 178.20 | 4.89 | 30.01 |
| 20 | 63.73 | 176.64 | 0 | 28.80 | 62.72 | 178.28 | 28.56 | 36.84 |
| 30 | 63.25 | 175.76 | 0 | 24.54 | 62.14 | 177.80 | 26.33 | 35.15 |

| Filler conc. (wt%) | HAp (<200 nm) | | | | *β*-TCP (0–50 μm) | | | |
|---|---|---|---|---|---|---|---|---|
| | $T_g$ (°C) | $T_m$ (°C) | Crystallinity (%) | $\Delta H_m$ (J $g^{-1}$) | $T_g$ (°C) | $T_m$ (°C) | Crystallinity (%) | $\Delta H_m$ (J $g^{-1}$) |
| 0 | 63.25 | 176.93 | 1.20 | 32.47 | 63.25 | 176.93 | 1.20 | 32.47 |
| 10 | 62.79 | 178.91 | 38.08 | 43.71 | n.d. | n.d. | n.d. | n.d. |
| 20 | 62.28 | 178.21 | 34.62 | 40.77 | 63.04 | 178.65 | 29.69 | 37.18 |
| 30 | 61.91 | 176.96 | 26.22 | 34.15 | n.d. | n.d. | n.d. | n.d. |

The melting point of the PLLA matrix increased by the addition of smaller particle sized HAp fillers. It is possible that the thermal movement of molecular chains of the polymer was restricted by the presence of the HAp particles during the endothermic melting process.

### 3.4 Mechanical properties

Tables 4 and 5 give the mean and standard deviation of flexural strength and modulus of elasticity for all PLGA and PLLA composites. It could be seen that the modulus of elasticity was improved when PLLA and PLGA were reinforced with all types of fillers. This is shown for the 5 μm particle size HAp PLGA composite in Fig. 3a. The optimum modulus of elasticity for both PLLA and PLGA was obtained when the 5 μm particle size HAp filler was used, 4.3 and 4.5 GPa respectively. This is firstly due to better interfacial adhesion between the matrices and particles. Secondly, it is possible that the particle distribution is better for this large-sized filler, compared to the smaller sized fillers. The flexural strength of manufactured profiles decreased, which is likely due to the inadequate adhesion of the filler particles to the polymer matrix and to the shape of the fillers. It is known that particulate fillers do not

**Table 4** Effects of different fillers with different concentrations on E-modulus, flexural strength and i.v. of PLGA (i.v. 3.3 dl $g^{-1}$))

| Filler conc. (wt%) | HAp (0–50 μm) | | | HAp (<5 μm) | | | HAp (<200 nm) | | | *β*-TCP (0–50 μm) | | |
|---|---|---|---|---|---|---|---|---|---|---|---|---|
| | i.v. (dl $g^{-1}$) | Strength (MPa) | Modulus (GPa) | i.v. (dl $g^{-1}$) | Strength (MPa) | Modulus (GPa) | i.v. (dl $g^{-1}$) | Strength (MPa) | Modulus (GPa) | i.v. (dl $g^{-1}$) | Strength (MPa) | Modulus (GPa) |
| 0 | 2 | 133 ± 2 | 3.3 ± 0.2 | 2 | 133 ± 2 | 3.3 ± 0.2 | 2 | 133 ± 2 | 3.3 ± 0.2 | 2 | 133 ± 2 | 3.3 ± 0.2 |
| 10 | 2.2 | 120 ± 3 | 3.5 ± 0.2 | 2.25 | 121 ± 5 | 3.4 ± 0.1 | 2.82 | 136 ± 5 | 3.7 ± 0.2 | n.d. | n.d. | n.d. |
| 20 | 2.3 | 115 ± 6 | 3.3 ± 0.2 | 2.44 | 123 ± 2 | 3.8 ± 0.2 | 2.6 | 129 ± 6 | 3.8 ± 0.2 | 2 | 113 ± 4 | 4 ± 0.2 |
| 30 | 2.4 | 100 ± 3 | 3.6 ± 0.2 | 2.44 | 118 ± 3 | 4.3 ± 0.2 | 2.36 | 105 ± 10 | 3.8 ± 0.6 | n.d. | n.d. | n.d. |

**Table 5** Effects of different fillers with different concentrations on E-modulus, flexural strength and i.v. of PLLA (i.v. 5.2 dl $g^{-1}$)

| Filler conc. (wt%) | HAp (0–50 μm) | | | HAp (0–5 μm) | | | HAp (<200 nm) | | | *β*-TCP (0–50 μm) | | |
|---|---|---|---|---|---|---|---|---|---|---|---|---|
| | i.v. (dl $g^{-1}$) | Strength (MPa) | Modulus (GPa) | i.v. (dl $g^{-1}$) | Strength (MPa) | Modulus (GPa) | i.v (dl $g^{-1}$) | Strength (MPa) | Modulus (GPa) | i.v. (dl $g^{-1}$) | Strength (MPa) | Modulus (GPa) |
| 0 | 2.93 | 131 ± 2 | 3.1 ± 0.06 | 2.93 | 131 ± 2 | 3.1 ± 0.06 | 2.93 | 131 ± 2 | 3.1 ± 0.06 | 2.93 | 131 ± 2 | 3.1 ± 0.06 |
| 10 | 2.9 | 121 ± 4 | 3.6 ± 0.3 | 3.45 | 115 ± 0.8 | 3.3 ± 0.1 | 2.23 | 124 ± 6 | 3.2 ± 0.2 | n.d. | n.d. | n.d. |
| 20 | 3.3 | 120 ± 4 | 3.8 ± 0.4 | 2.45 | 122.5 ± 2 | 4 ± 0.2 | 1.5 | 109 ± 3 | 3.5 ± 0.4 | 2.4 | 123 ± 2 | 3.6 ± 0.3 |
| 30 | 3.24 | 106 ± 5 | 3.8 ± 0.4 | 2.3 | 119 ± 3 | 4.5 ± 0.2 | 1.9 | 91 ± 5 | 3.3 ± 0.3 | n.d. | n.d. | n.d. |

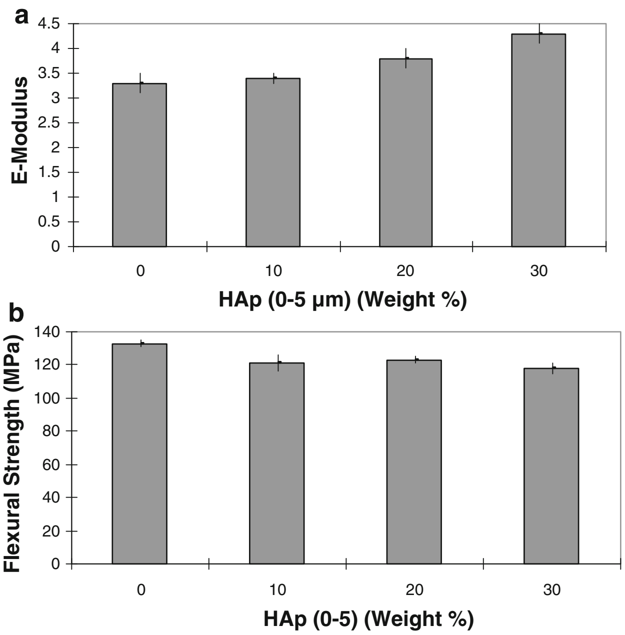

**Fig. 3** Modulus of elasticity (**a**) and flexural strength (**b**) for PLGA 5 µm particle size HAp at different filler loadings

hinder crack propagation through a composite material as effectively as fiber-shaped fillers. The present values for flexural strength correspond well to the average values of particulate filler composite made of thermoset resins. These values are on average, one-third of the flexural strength of compact bone. Therefore, the composite tested in this study cannot in its present form, be used in load bearing applications. This is especially so since it is likely that water saturation of the composite would further reduce the strength. The modulus of elasticity was improved in profiles with 20 wt% $\beta$-TCP to approximately 4.0 GPa but the flexural strength decreased to 113 MPa in comparison to the pure polymers. It is evident that the filler ratio for obtaining both high modulus of elasticity and strength in melt blending of $\beta$-TCP filler should not exceed 20 wt%.

### 3.5 Specimen morphology

The best illustration of the fracture surfaces was obtained with a SEM magnification of 1500×. The fracture surfaces for the PLGA and PLLA composites with 10–30 wt% HAp

**Fig. 4** SEM micrographs of fracture surfaces for PLGA respective PLLA composites with **a** 10 wt%, **b** 20 wt%, **c** 30 wt% HAp filler content

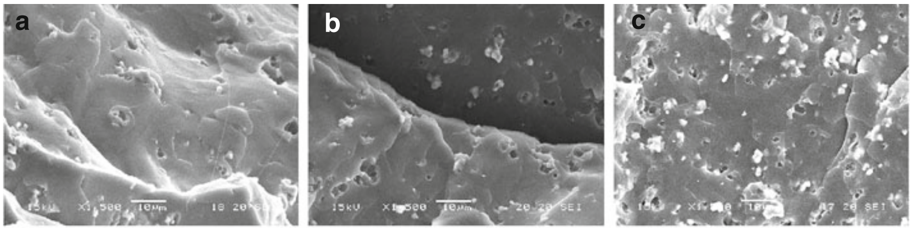

PLGA + HAp (0-50 µm)

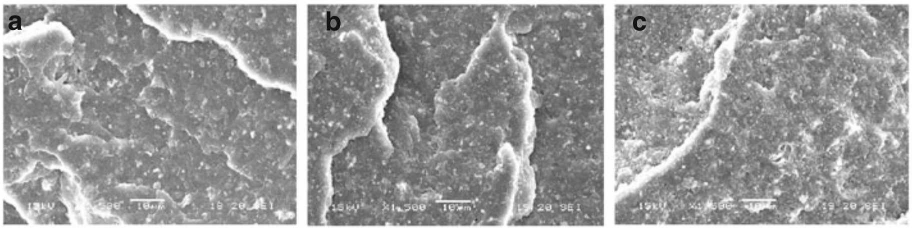

PLGA + HAp (0-5 µm)

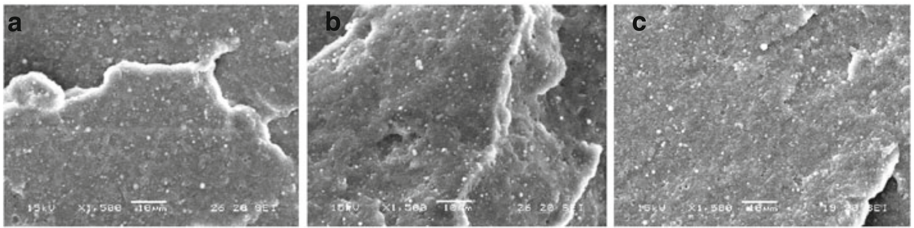

PLGA + HAp (200 nm)

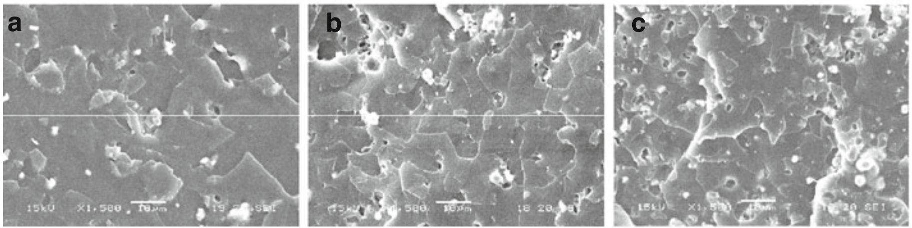

PLLA+HAp (0-50 µm)

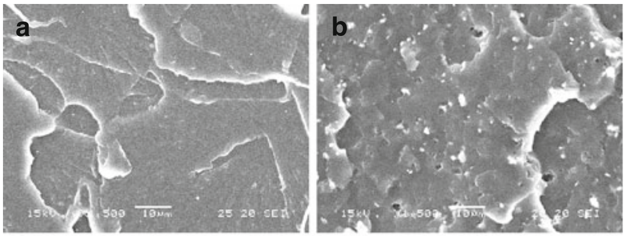

PLGA + β-TCP (0-50 μm)

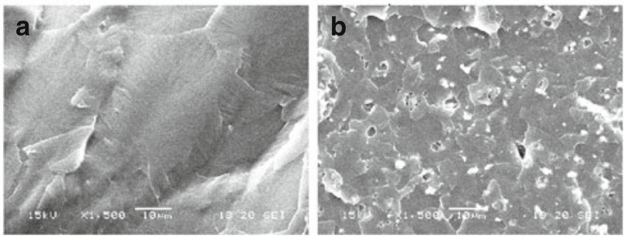

PLLA + β-TCP (0-50 μm)

**Fig. 5** SEM micrographs of fracture surfaces for PLGA respective PLLA composites, **a** neat profiles, **b** 20 wt% $\beta$-TCP filler content

are shown in Fig. 4. Similar micrographs are shown for $\beta$-TCP composites in Fig. 5. The presence of fillers larger than 50 μm in the $\beta$-TCP composites can be seen. The gradual increase in the filler amount was clearly seen. A complete homogenous distribution of the fillers in the polymer matrices was witnessed, especially for the specimens compounded with 200 nm particle size and 5 μm particle size microsphere particles. Some agglomeration of fillers with 50 μm particle size was evident for less homogenous profiles with large filler particle size. Although few agglomerations could be seen, the most uniformly distributed particles were observed for the 200 nm particle size HAp reinforced composites. The particles were loosely bound to the polymer matrix which helped explain the lower flexural strength discussed above.

Due to the risk of thermal degradation effects during the composite production process, the residence time of polymer in the extruder was adjusted to just 2 min. No preparatory mixing procedure was needed, which led to a satisfactory filler distribution in the polymer matrix.

### 3.6 Thermogravimetric analysis

The continuous processing of the profiles by gradual feeding of the polymer-filler mixture could lead to variations in the filler content in different sections of the extruded profiles. This would lead to inhomogeneous filler distribution along the profiles and cause wide variations in composite properties. By thermogravimetric analysis it was possible to determine the content of the inorganic filler in the composites. Specimens from the starting, middle and end portions of each profile were analysed using TGA. Typical TGA scans for specimens taken from different profile parts of the PLGA composite with 20 wt% 5 μm particle size HAp are shown in Fig. 6. Similar results indicated an homogeneous filler distribution in all profiles. The obtained data is given in Table 6 for the PLGA and PLLA composites. Interpretation of the data from the TGA curves clearly illustrated that thermal processing of polymer granules and filler powders with a 2 min residence time allowed for homogenous profiles to be produced. The deviation of filler concentration in all parts of profiles was ±2 wt% and the actual concentration was 3–5 wt% less than the intended amount. Distribution of fillers with particle size 0–50 μm was not as homogenous as the nanoparticles and the 0–5 μm particles. The TGA results were confirmed by the SEM images which showed that large particles were agglomerated and did not disperse in all

**Fig. 6** TGA curves recorded at 20°C min$^{-1}$ under nitrogen flow for PLGA + 20 wt% 5 μm HAP from first, middle and end part of profile

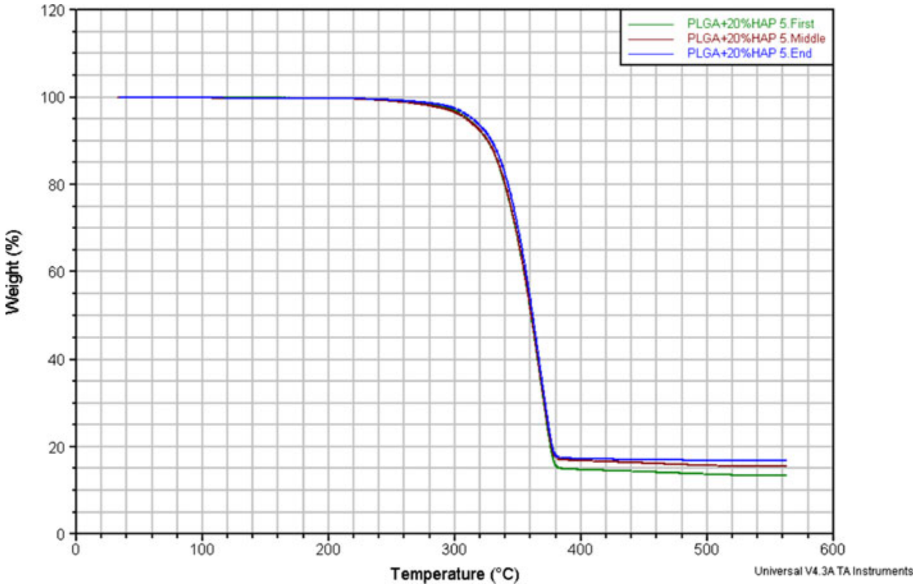

**Table 6** TGA estimated filler content compared to the intended filler content in PLGA and PLLA composites

| Intended filler content (wt%) | Real filler content (wt%) | | | |
|---|---|---|---|---|
| | HAp (0–50 μm) | HAp (5 μm) | HAp (<200 nm) | β-TCP (0–50 μm) |
| PLGA | | | | |
| 10 | 7.71 | 7.47 | 10.43 | – |
| 20 | 17.35 | 16.28 | 17.34 | 18.97 |
| 30 | 28.37 | 27.04 | 28.19 | – |
| PLLA | | | | |
| 10 | 5.10 | 9.12 | 10.16 | – |
| 20 | 14.24 | 15.44 | 16.23 | 16.45 |
| 30 | 24.98 | 25.48 | 25.39 | – |

parts of polymer matrix. The filler concentration in PLGA was more close to the intended amount compared to PLLA. This was due to the presence of more PLLA residuals from previous runs and the dilution of these residuals when following runs were performed.

## 4 Conclusions

More than one meter in length and 2–3 mm diameter, homogenous smooth profiles were produced in one compounding batch. Optimum processing conditions for melt extruding of PLLA and PLGA were determined, which are applicable for industrial scale. Minimum degradation was observed in compounding (PLGA) (i.v. 3.3–2.6) and no significant changes were seen in $T_m$ and $T_g$. The addition of HAp and β-TCP improved the modulus of elasticity up to 4.5 GPa and reduced the flexural strength. With reasonable mechanical properties, a high rate of degradation in compounding PLLA (i.v. 5.5–2.5) was witnessed. Filler agglomeration in polymer matrices with 50 μm particle sizes was observed. The greatest improvement in E-modulus and the slightest reduction in flexural strength occurred in profiles that were reinforced with HAp particle size, 0–5 μm.

Due to the potential effects of thermal degradation, the residence time of the polymer in the extruder was adjusted to a minimum of 2 min. Despite the lack of preparatory mixing, a highly desirable filler distribution was obtained in the polymer matrices.

**Acknowledgments** Deepest gratitude is payable to the members of the Newbone EU FP6 project for their advice, interpretations and suggestions. The authors are thankful to Dr. Riina Mattila, University of Turku, Finland for her sincere, outstanding help and support in scanning electron microscopy and mechanical tests.

## References

1. Dee KC, Puleo DA, Bizios R. An introduction to tissue-biomaterial interactions. Hoboken: Wiley; 2003.
2. Anderson JM, Shive MS. Biodegradation and biocompatibility of PLA and PLGA microspheres. Adv Drug Deliv Rev. 1997;28(1):5–24.
3. van de Velde K, Kiekens P. Biopolymers: overview of several properties and consequences on their applications. Polym Test. 2002;21(4):433–42.
4. Athanasiou KA, Agrawal CM, Barber FA, Burkhart SS. Orthopaedic applications for PLA-PGA biodegradable polymers. Arthroscopy. 1998;14(7):726–37.
5. Pillin I, Montrelay N, Grohens Y. Thermo-mechanical characterization of plasticized PLA: is the miscibility the only significant factor? Polymer. 2006;47(13):4676–82.
6. Gupta B, Revagade N, Hilborn J. In vitro degradation of dry-jet-wet spun poly(lactic acid) monofilament and knitted scaffold. J Appl Polym Sci. 2007;103(3):2006–12.
7. Vasenius J, Helevirta P, Kuisma H, Rokkanen P, Törmälä P. Absorbable self-reinforced polyglycolide (SR-PGA) screws for the fixation of fractures and osteotomies—strength and strength retention in-vitro and in-vivo. Clin Mater. 1994;17(3):119–23.
8. Vert M, Schwach G, Engel R, Coudane J. Something new in the field of PLA/GA bioresorbable polymers? J Control Release. 1998;53(1–3):85–92.
9. Nazhat SN, Kellomäki M, Törmälä P, Tanner KE, Bonfield WS. Dynamic mechanical characterization of biodegradable composites of hydroxyapatite and polylactides. J Biomed Mater Res. 2001;58(4):335–43.
10. Belbella A, Vauthier C, Fessi H, Devissaguet JP, Puisieux F. In vitro degradation of nanospheres from poly(D,L-lactides) of different molecular weights and polydispersities. Int J Pharm. 1996;129(1–2):95–102.
11. Lai WC, Liau WB. Thermo-oxidative degradation of poly(ethylene glycol)/poly(L-lactic acid) blends. Polymer. 2003;44(26):8103–9.
12. Lin PL, Fang HW, Tseng T, Lee WH. Effects of hydroxyapatite dosage on mechanical and biological behaviors of polylactic acid composite materials. Mater Lett. 2007;61(14–15):3009–13.
13. Mathieu LM, Bourban PE, Månson JAE. Processing of homogeneous ceramic/polymer blends for bioresorbable composites. Compos Sci Technol. 2006;66(11–12):1606–14.
14. Pluta M. Melt compounding of polylactide/organoclay: structure and properties of nanocomposites. J Polym Sci Polym Phys. 2006;44(23):3392–405.
15. Xu X, Chen X, Liu A, Hong Z, Jing X. Electrospun poly(L-lactide)-grafted hydroxyapatite/poly(L-lactide) nanocomposite fibers. Eur Polym J. 2007;43(8):3187–96.
16. Passerini N, Craig DQ. An investigation into the effects of residual water on the glass transition temperature of polylactide microspheres using modulated temperature DSC. J Control Release. 2001;73(1):111–5.
17. Park TG. Degradation of poly(lactic-co-glycolic acid) microspheres—effect of copolymer composition. Biomaterials. 1995;16(15):1123–30.
18. Porjazoska A, Karal-Yilmaz O, Kayaman-Apohan N, Cvetkovska M, Baysala BM. Biocompatible polymer blends of poly(D,L-lactic acid-co-glycolic acid) and triblock PCL-PDMS-PCL copolymers: their characterizations and degradations. J Croat Chem Acta. 2004;77(4):545–51.
19. Weir NA, Buchanan FJ, Orr JF, Farrar F, Boyd A. Processing, annealing and sterilisation of poly-L-lactide. Biomaterials. 2004;25(18):3939–49.

20. Niiranen H, Törmälä P. Bioabsorbable polymer plates coated with bioactive glass spheres. J Mater Sci Mater Med. 1999; 10(12):707–10.
21. Ehrenfried L, Patel M, Cameron R. The effect of tri-calcium phosphate (TCP) addition on the degradation of polylactide-co-glycolide (PLGA). J Mater Sci Mater Med. 2008;19(1):459–66.
22. Lee KY, Blaker JJ, Bismarck A. Surface functionalisation of bacterial cellulose as the route to produce green polylactide nanocomposites with improved properties. Compos Sci Technol. 2009;69(15–16):2724–33.
23. Demir S, Ogan A, Kayaman-Apohan N. Intrinsic factor and vitamin B12 complex-loaded poly[lactic-co-(glycolic acid)] microspheres: preparation, characterization and drug release. Polym Int. 2008;57(2):372–7.